TEST SYSTEM FOR THE INVESTIGATION OF THE SYNERGY POTENTIAL OF SOLAR COLLECTORS AND BOREHOLE HEAT EXCHANGERS IN HEAT PUMP SYSTEMS

Peter Pärisch, Maik Kirchner, Wolfgang Wetzel, Sheila Voß, Rainer Tepe

Institut für Solarenergieforschung Hameln GmbH (ISFH), Emmerthal (Germany)

1. Introduction

The wide variety of solar assisted heat pump systems makes it difficult to assess the energetic behavior and to find optimized solutions. In order to come to a deeper understanding, scientists from different subjects are cooperating with the aim to analyze the synergy effects of solar heat and heat pumps with borehole heat exchangers (BHE).

The research project, which is funded by the European Union and the Federal State of Lower Saxony, is running from September 2010 until August 2013. Several industry partners from Lower Saxony will support the project with regard to the technical feasibility and the market relevance.

The Geoscience Centre of the Georg-August-University of Göttingen and the State Authority for Mining, Energy and Geology of Lower Saxony will investigate the ground heat transfer issues, carrying out detailed geologic and hydro-geologic experiments and simulations.

Within a field investigation of realized ground-coupled heat pump systems Ostfalia – University of Applied Sciences of Wolfenbüttel will analyze the potential efficiency improvement by optimizing the heat supply system of 8 to 10 existing solar assisted ground-coupled heat pump systems. System simulations will complete the evaluation of measured data.

The goal of ISFH is to analyze different system concepts by TRNSYS simulations and carry out reproducible experiments at the new test system. The setup of the test system and first experiments with the borehole heat exchangers are presented in this paper.

2. New test system at ISFH

ISFH has installed a variable test facility, consisting of a ground source circuit, two different heat pumps, which may be operated alternatively or simultaneously, and three programmable high precision modules, which allow emulating solar collector circuits, domestic hot water and space heating circuits, see Fig. 1.

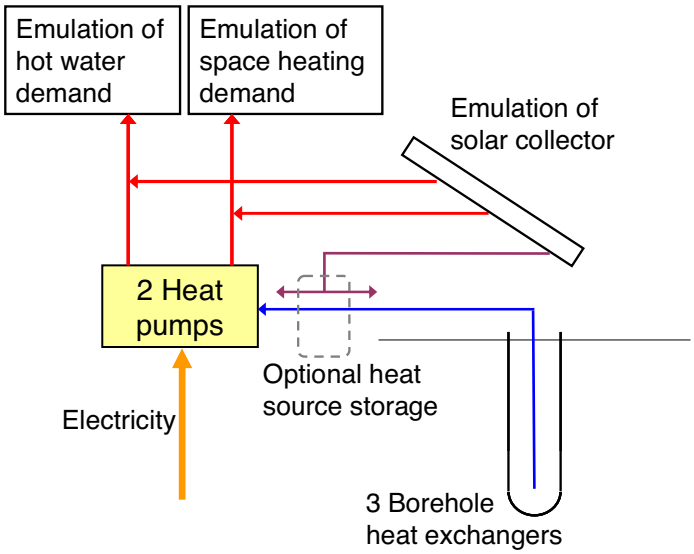

Fig. 1: Simplified scheme of the test facility at ISFH

This test system allows investigating different solar and ground-coupled heat pump combinations, where especially the solar heat may be directed

a) to the ground,

b) onto the evaporator of the heat pump,

c) into a storage at the source side

d) or directly to the demand side,

depending on its current temperature level and energy saving potential.

Heat flow rates into or out of various subsystems like heat pump, solar circuit, borehole heat exchanger, heat storage may be measured with high accuracy sensors for mass flow rates and temperatures. Temperature sensors are calibrated and have a standard uncertainty of 0.064 K. Mass flow rate sensors are calibrated as

well and have a standard uncertainty of 0.1 to 0.2 %. Electric energy is measured for the compressor and for auxiliary consumers.

As Fig. 2 shows, the ground source test field consists of three borehole heat exchangers (SW, SN, SO) placed in the corners of an isosceles triangle each with a depth of about 70 m. Furthermore, the borehole field comprises a temperature-measuring borehole (TW) 1 m next to the left BHE and two ground water measuring wells (BM, BS) in order to determine the permeability in different layers of the ground. Every borehole heat exchanger and the temperature-measuring borehole are equipped with at least one temperature chain consisting of 10 Pt100 sensors. These measure the temperature from a depth of 7 m to 70 m in a distance of 7 m. On top of each BHE in a depth of about 1.2 m the fluid temperatures are measured in the elbow fittings at the inlet into the horizontal pipes. So, the actual length of the BHEs (see Fig. 2) is less than their depth due to overlying ground and weights at the end of the BHEs.

Additionally, all 6 boreholes are provided with a distributed temperature system (DTS) based on fiber optic cable. The DTS system allows the measurement in the ground with a spatial resolution of 1 m. In total, over 1700 m of fiber optic cable are installed in the ground. The BHEs are realized as double U-pipes, made of cross-linked polyethylene, which may be operated up to 95 °C. In a step size of one meter, spacers have been assembled and the measuring cables were fixed with tape. The BHE were grouted with enhanced backfilling material having a thermal conductivity of $k \approx 2\ W \cdot m^{-1} \cdot K^{-1}$.

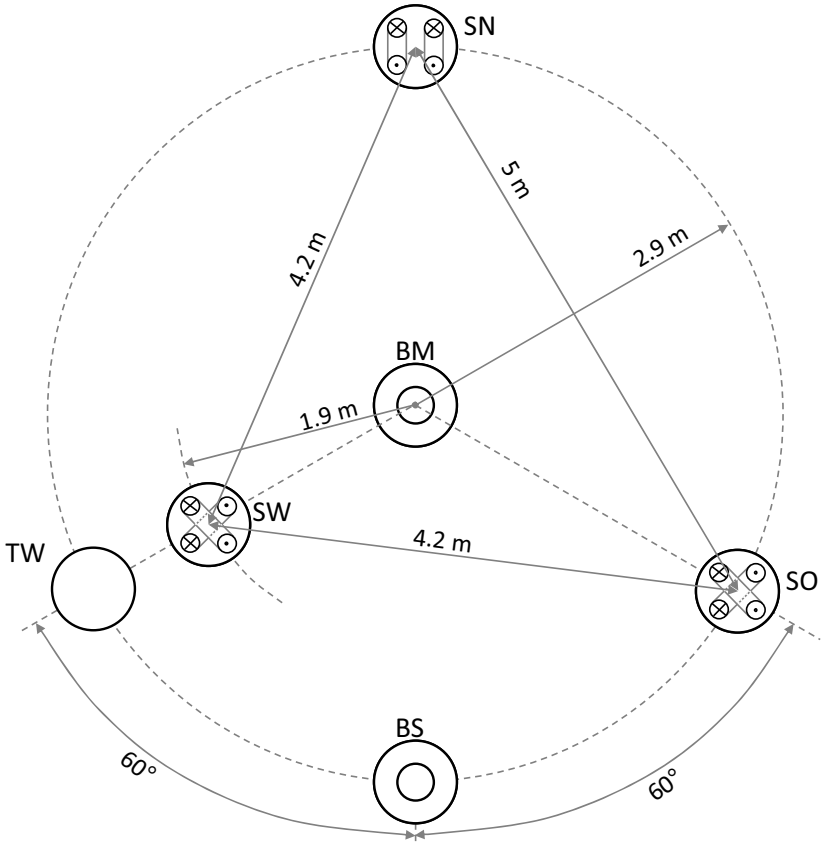

Name	Type	Pt100 chain	DTS-loop	Length of BHE	Depth of borehole	Max. deviation of vertical line
SN	BHE	2	2	68,5 m	71 m	0.27 m
SO	BHE	1	1	69,3 m	71 m	0.38 m
SW	BHE	1	1	69,5 m	71 m	0.15 m
BM	Well	0	1	67	67 m	0.53 m
BS	Well	0	1	67	70 m	0.89 m
TW	Temperature	1	1	68,8 m	70 m	0.15 m

Fig. 2: Detailed map of test field at ISFH

The boreholes were drilled with a double-head rotary drilling equipment aiming at a low deviation from the vertical line. With the double head the casing and drilling rod operate at the same time. The 165 mm steel casing is lowered to the final depth of the boreholes and removed after borehole completion. The deviations of the boreholes from the vertical line were measured for quality reasons. The maximum deviation appeared at the south well (BS) with 0.89 m (see Fig. 2 and Fig. 3).

Very low deviations were achieved at the borehole heat exchangers, which is very important for the investigation of their interaction.

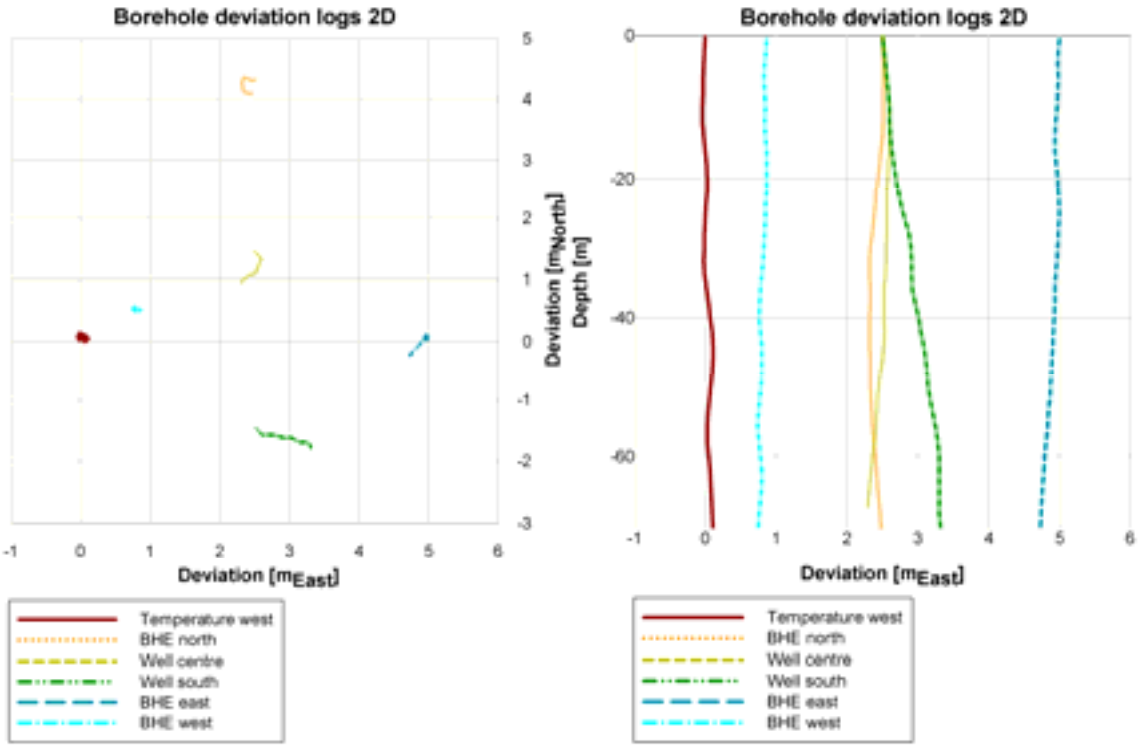

Fig. 3: Measured borehole deviations of the test field (left: view from above, right: vertical section)

In order to assess the boreholes, geologic measurements like gamma-ray, density, salinity, neutron-log were performed. The ground water level was identified to be at 28 m.

The State Authority for Mining, Energy and Geology of Lower Saxony (LBEG) analyzed the drilling mud of every meter chemically and geologically.

The profiles of the drillings show a sequence of sandstone belonging to the Upper Triassic (Carnian) Stuttgart-Formation and below an alternating sequence from marlstone, claystone and dolomite. The complete sequence could be dated to the upper Julium subunit of the Cranium.

Fig. 4 shows the ground layers, which show mainly two sections. Down to 13 m below ground there is sandstone. From 13 m to 70 m a mixture of claystone and marlstone with slightly varying composition has been found.

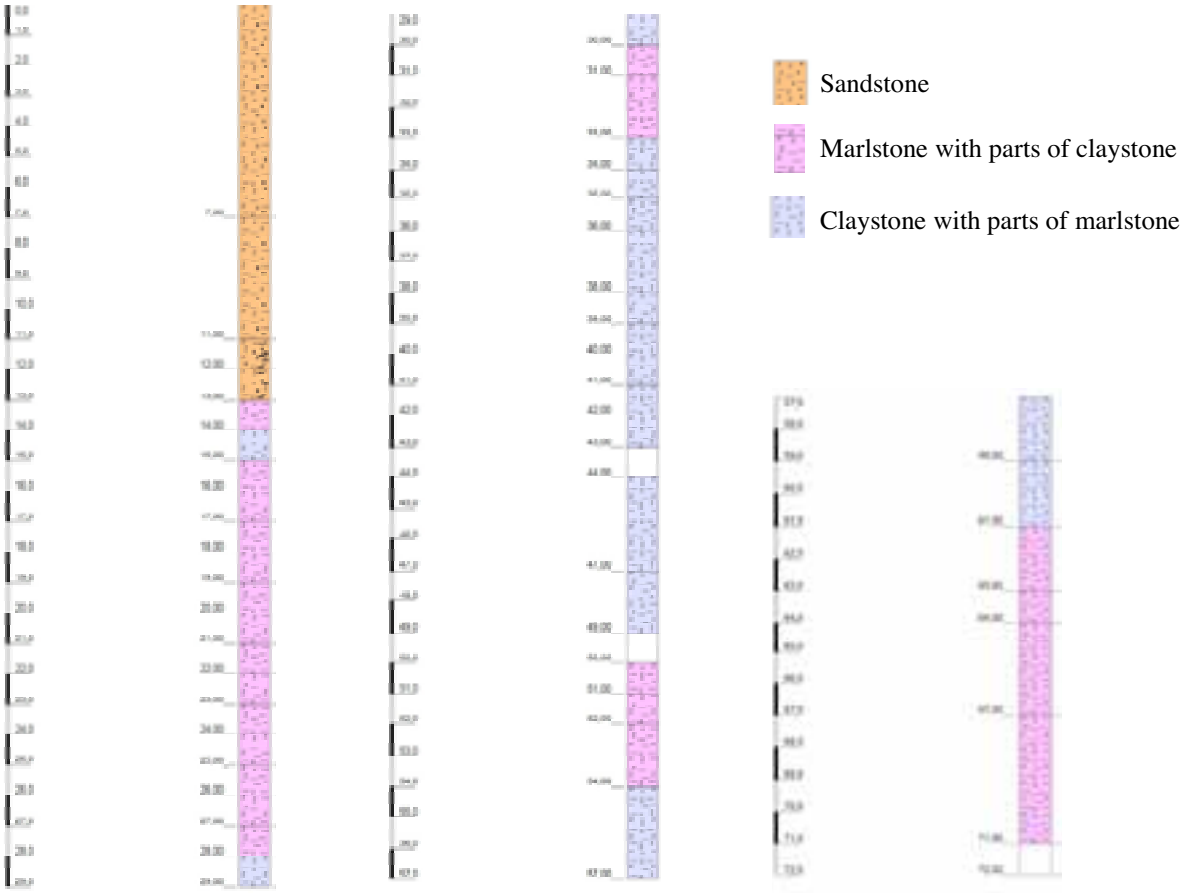

Fig. 4: Brief documentation of the ground layers at the test facility (modeled after: LBEG)

3. Properties of ground and borehole heat exchangers

Different tests with borehole heat exchangers were and will be carried out and compared to simulations. For that purpose it is important to know the starting conditions in the ground and the ground properties.

Usually TRNSYS types are initialized with the undisturbed ground temperature according to (KUSUDA & ACHENBACH, 1965), so this empiric approach has to be adapted. The measured undisturbed ground temperatures in different depths can be described by equation 1 from (KUSUDA & ACHENBACH, 1965), which was here supplemented with the geothermal gradient:

$$\vartheta(t,z) = \overline{\vartheta} - \hat{\vartheta} \cdot \exp\left[-z \cdot \left(\frac{\pi}{T \cdot a}\right)^{1/2}\right] \cdot \cos\left\{\frac{2\pi}{T} \cdot \left[t - t_0 - \frac{z}{2} \cdot \left(\frac{T}{\pi \cdot a}\right)^{1/2}\right]\right\} + z \cdot \frac{d\vartheta}{dz} \qquad \text{(eq. 1)}$$

With: $\vartheta(t,z)$ Undisturbed ground temperature at specific time t and depth z

$\overline{\vartheta}$ Long-term ambient air temperature, at location of ISFH 9.73 °C

$\hat{\vartheta}$ Amplitude of the ambient air temperature, at location of ISFH 12 K

z Depth [m]

T Periodic time of the sinusoidal temperature curve (365 d)

t Time, at ISFH 30 d

t_0 Phase shift between the time with minimal ambient air temperatures and 1. January [d]

a Thermal diffusivity of the ground, here [m²/d]

The measured geothermal gradients between 20 and 70 m at the boreholes at ISFH are about 1.1 K/100 m.

Fig. 5 shows the comparison of equation 1 with measured temperatures from two different days after the installation. The visible offset of about 0.7 K may be caused by the ambient air temperature that has been measured on top of a building nearby with a height of about 7 m. Additionally, equation 1 with a hypothetic mean ambient air temperature of 10.4 °C is plotted in Fig. 5.

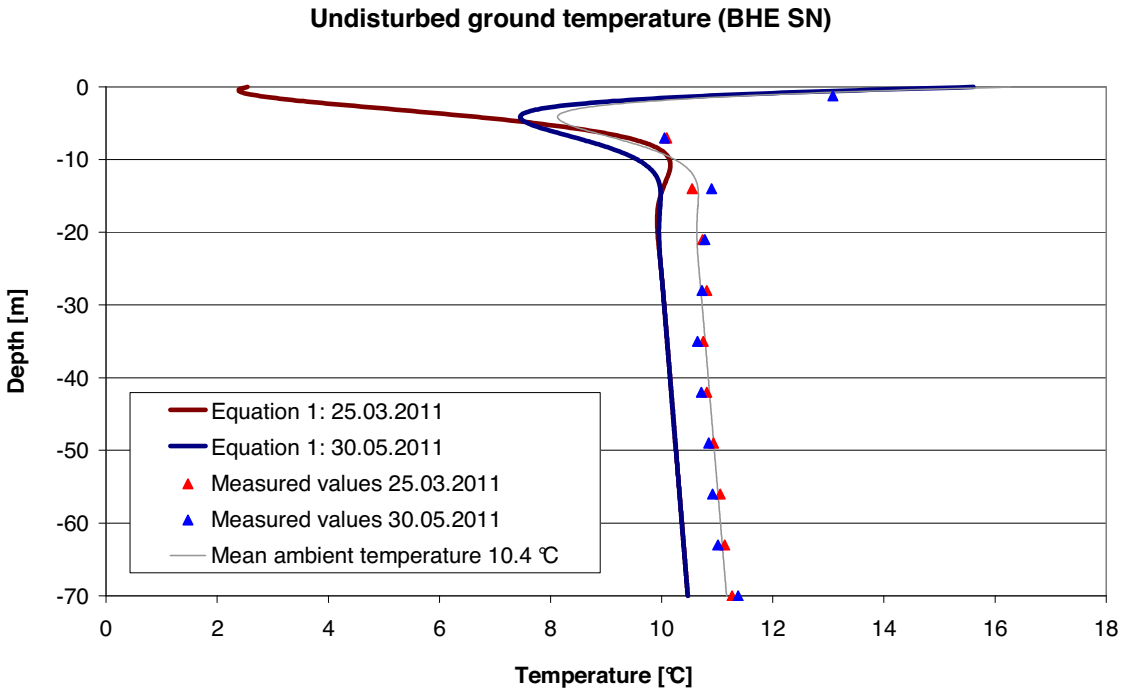

Fig. 5: Comparison of measured and expected ground temperatures according to eq. 1

Ground properties like thermal conductivity of the ground and thermal resistance of BHE can be obtained from geothermal response tests, as described e. g. in (GEHLIN, 2002). Fig. 6 shows the measured values of the mass flow rate, the heat flow rate and the mean fluid temperature of the GRT of the borehole heat exchanger SO.

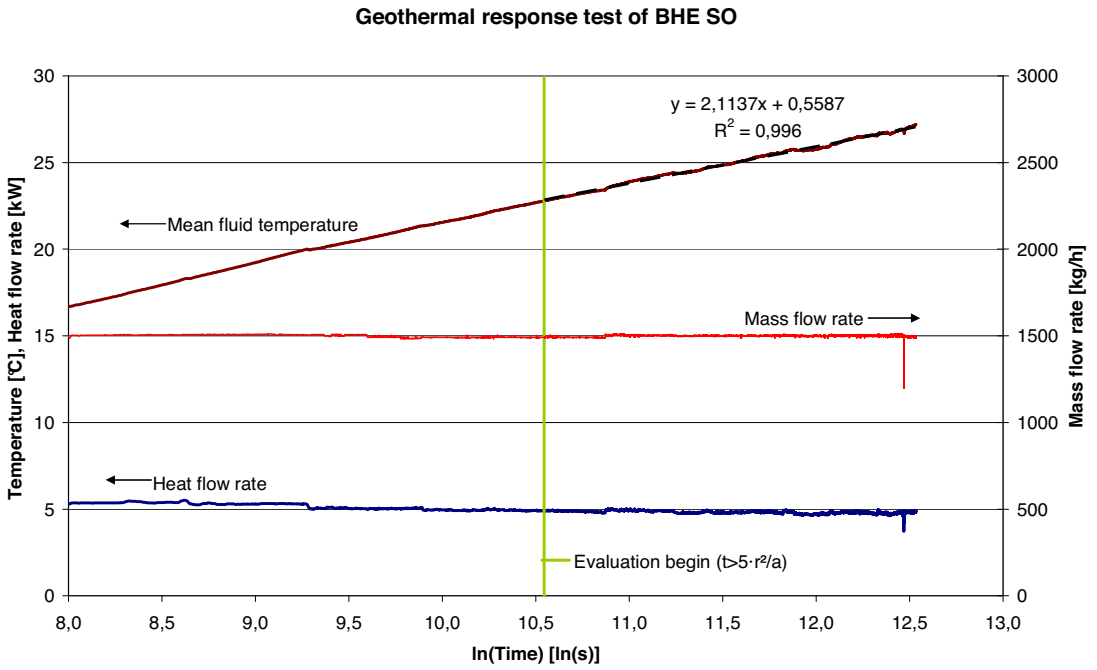

Fig. 6: Measured data of the geothermal response test of BHE SO

Tab. 1 gives an overview of the determined borehole properties from the geothermal response tests.

Tab. 1: Thermal conductivity and borehole thermal resistance for the three BHEs

Borehole heat exchanger	Thermal conductivity k	Borehole thermal resistance R_b
SN	2.25 $W \cdot m^{-1} \cdot K^{-1}$	0.118 $m \cdot K \cdot W^{-1}$
SO	2.61 $W \cdot m^{-1} \cdot K^{-1}$	0.100 $m \cdot K \cdot W^{-1}$
SW	2.29 $W \cdot m^{-1} \cdot K^{-1}$	0.070 $m \cdot K \cdot W^{-1}$

Although construction and installation of the borehole heat exchangers are identical, a high deviation in R_b can be seen. The deviation in thermal conductivity is remarkable as well because the distance between the BHEs is rather small (4-5 m). This is assumed to be caused by different ground water permeability coefficients. The rock system at the test site is fractured so that ground water can circulate in the network of fissures. The fissures are not equally distributed which means the contact zone of ground water to the BHE differs for each borehole and depth. This affects the temperatures in different layers.

This can be analyzed more precisely using the DTS system (see Fig. 7). First, the match between the DTS system and the Pt100 chain is remarkable. Second, the regeneration happens with different velocities at different layers. For example, the temperature in a depth of 7, 37, 56 and 70 m sinks after the GRT (left) more rapidly. This can be seen after the heat extraction test (see Fig. 7, right diagram) as well.

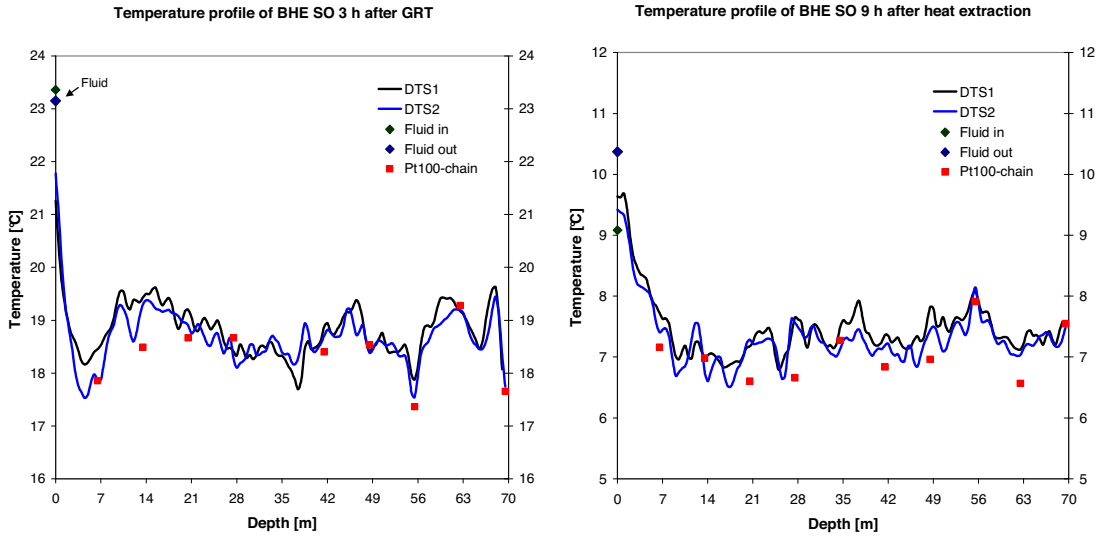

Fig. 7: Comparison of DTS and Pt100 chain 3 h after GRT (left) and 9 h after heat extraction (right) on the BHE SO

With the detailed temperature information of the ground it is possible to reach designated ground temperature conditions, like undisturbed ground temperature, before starting a new test. In order to avoid a temperature drift in the ground the energy balance of the BHEs can be set to zero after every test, like proposed in (KOENIGSDORFF et al., 2010).

The different strategies for improving the COP by solar thermal heat on the source side

- by directly increasing the evaporator inlet temperature,
- by leading the solar heat via the BHE to the evaporator side or
- by merging both heat sources circuits in a storage or manifolds

will be investigated during the project. Aspects of BHE fields will be investigated as well, which includes e. g. the opportunities for storing solar heat over a longer period and the regeneration of BHE fields, which have been deep-discharged over a long period.

4. Heat pump testing

TRNSYS simulations show that regeneration of the ground with solar heat increases the mean evaporator inlet temperature. This is of course depending on the length of the BHE, the heat load, the ground properties and the collector area. (BERTRAM et al., 2011)

Fig. 8 shows an example for the evaporator inlet temperature in the course of a year.

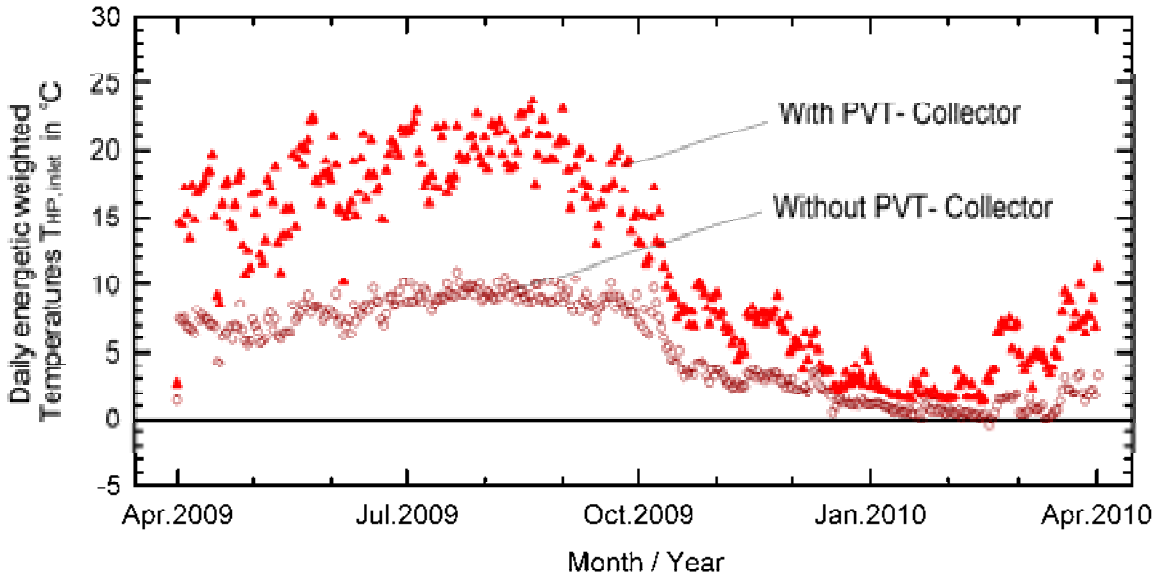

Fig. 8: Daily average energetic weighted temperatures at the heat pump inlet $T_{HP,inlet}$ for a pilot system (user heat demand 35 MWh/a, 12 kW heat pump, 39 m² PVT-Collector, 3x75 m coaxial BHE) in the first year of operation (with PVT-Collector: validated simulated data; without PVT-Collector: extrapolated data) (BERTRAM et al., 2011)

Fig. 8 shows, that the solar heat increases the evaporator inlet temperature. A significant difference appears during the summer months that typically have a rather low COP. Meanwhile in wintertime the difference is only a few degrees, however representing the largest fraction of annual energy demand. Over the year, the energetic weighted increase of the evaporator inlet temperature is about 3 K, which leads to an electricity saving of about 10 %.

One important question may be derived from Fig. 8, i. e. how does the heat pump's COP react to different inlet temperatures, and what may be concluded from this with regard to system interconnection.

For this purpose, the test system allows the measurement of characteristic curves of heat pumps according to DIN EN 14511. Equation 2 shows the complete equation for COP for a heat pump with external circulation pumps (DIN EN 14511-3, 2008).

$$COP = \frac{\dot{Q}_{Cond} + P_{pump\_Cond}}{P_{el,Comp} + P_{el,Contr+Safety} + P_{pump\_Cond} + P_{pump\_Eva}} \qquad \text{(eq. 2)}$$

For one heat pump different source and sink temperatures at different mass flow rates have been investigated, which is shown in Fig. 9.

It is well-established that high source temperatures and low sink temperatures promote heat pump efficiency. The COP shows almost a linear dependency of the source temperature. But at higher temperatures than 15 °C and 20 °C respectively the characteristic curves at sink temperatures of 50 °C and 60 °C respectively feature a modest gradient. This effect seems to shift with higher sink temperatures to higher source temperatures. This means that solar heat at higher temperatures is useful for operation periods of the heat pump to provide high sink temperatures.

The dependency on evaporator flow rate is rather low. Following that coupling of the solar collector loop to the heat source loop may influence the flow rate without affecting the COP.

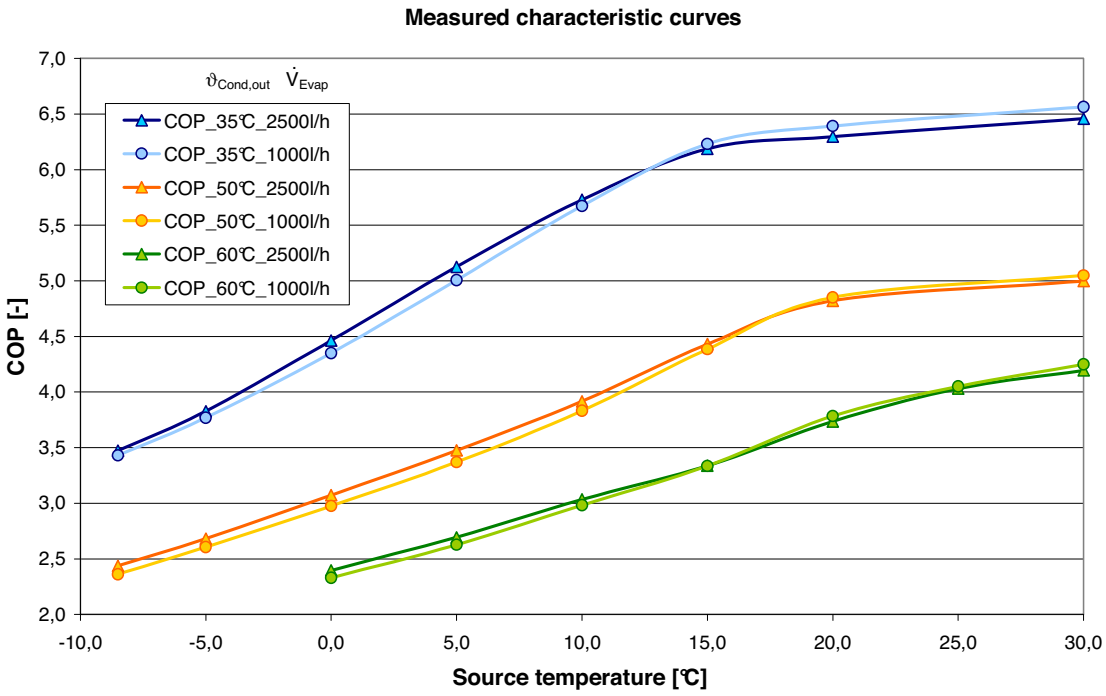

Fig. 9: Measured characteristic curves of a heat pump at 3 different heat sink temperatures, each with 2 evaporator flow rates

The curves for different evaporator side flow rates show, that there is nearly no effect even with this rather high variation (the nominal flow rate is 1900 l/h). It is not surprising, that increasing source temperatures and decreasing sink temperatures lead to higher COP values. However, it may be seen, that above a certain temperature the COP stays approximately constant, what is in contradiction to the Carnot factor. To analyze this, the quality grade of the heat pump, which is the measured COP divided by the Carnot factor at the measured temperatures, has been determined. A quality grade of 1 would represent an ideal heat pump with the efficiency of the Carnot process.

It can be seen in Fig. 10 that this ground-coupled heat pump is optimized for temperatures between 0 and 15 °C. For higher evaporator temperatures, which may be caused by solar input to the evaporator, the quality grade decreases rapidly.

If the source flow rate is reduced from 2.5 (nominal value is 1.9) to 1.0 m³/h, the quality grade reduces only about 1-3 %-points.

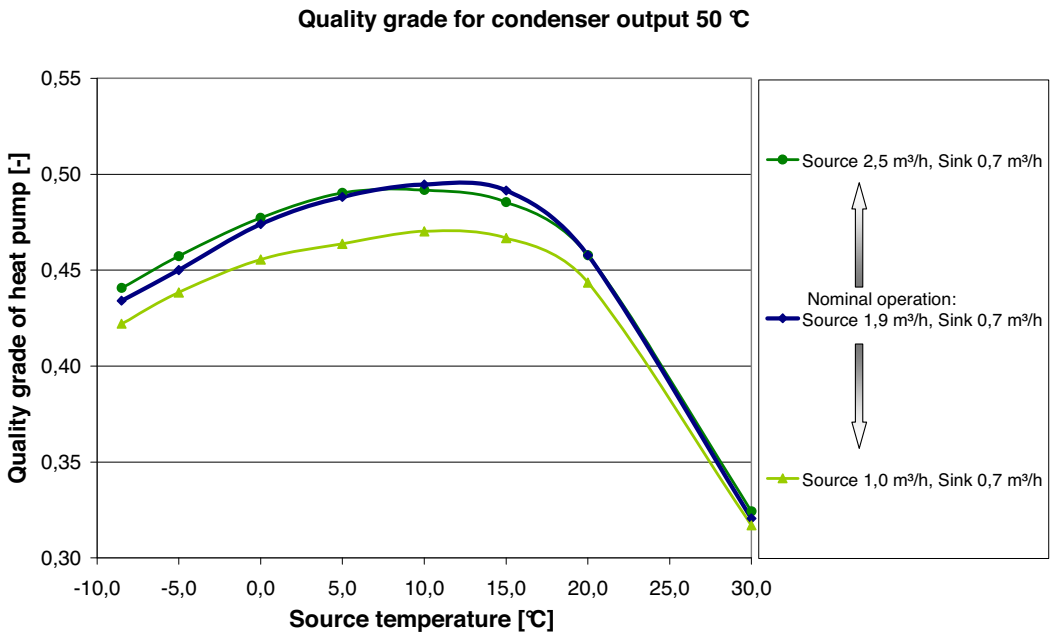

Fig. 10: Measured heat pump quality grade vs. source temperature, with different source flow rates and constant sink outlet temperature

Fig. 11 shows that the quality grade is more sensitive to sink flow rate if the condenser output is kept constant (here 50 °C). This is due to the fact that the mean condenser temperature sinks with decreasing flow rate. Vice versa Fig. 11 shows that a low return temperature of the load is more important with low flow rates. This has a high impact on COP and quality grade.

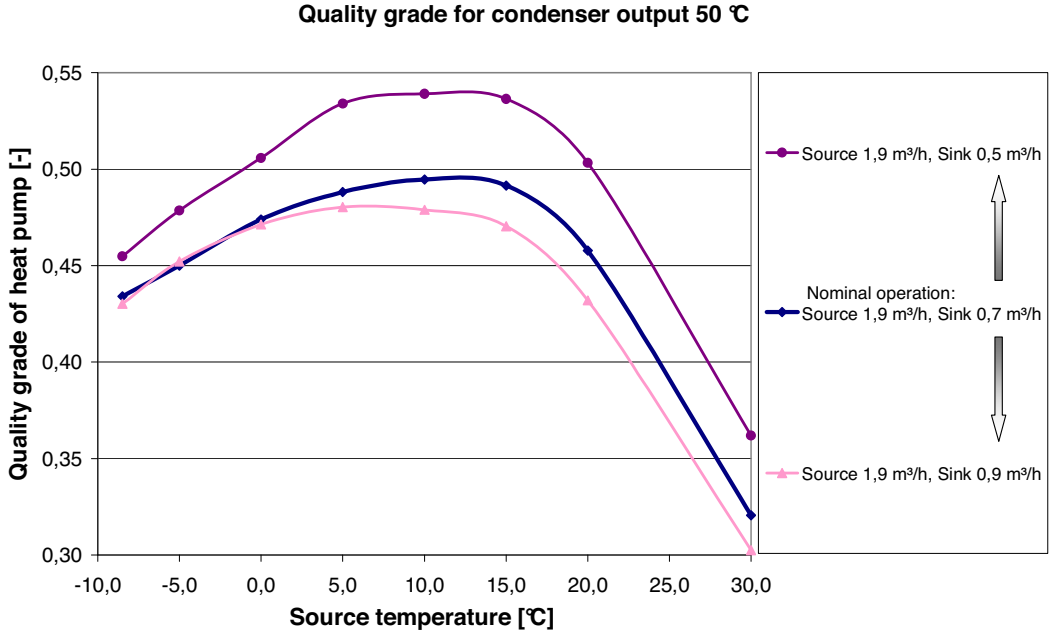

Fig. 11: Measured heat pump quality grade vs. source temperature, with different sink flow rates and constant sink outlet temperature

The examples discussed show that the test facility for heat pumps allows for example the testing of improved heat pumps, which are designed for the combination with solar heat.

The measurements will be compared with computer simulations in order to improve the heat pump models for example for variable mass flow rates.

5. Conclusion and outlook

ISFH has built a variable test facility with three borehole heat exchangers for testing complete brine-water heat pump systems. The test facility is equipped with high quality sensors in the ground and in the system.

The test facility allows carrying out tests on complete systems, including dynamic load and solar heat flow rates. Subsystems may be investigated in details and will be compared with simulations. E. g., the behavior of a borehole regenerated through the day and discharged during the night is of interest as well as the behavior of a heat pump at higher source temperature or varying fluid flow rates.

Furthermore, the test facility enables to test different strategies and operating modes for the input of solar heat to the source side and the sink side. One question will be, whether a lower heat flow is directed to the sink side or a higher amount is used on lower temperature level at the source side, at a given collector and heat pump configuration.

6. Acknowledgements

The project “Hocheffiziente Wärmepumpensysteme mit Geo- und Solarthermie- Nutzung” (High-efficient heat pump systems with geothermal and solar thermal energy sources, short name: Geo-Solar-WP) is funded by the European Union (European Regional Development Fund) and the Federal State of Lower Saxony. The work has been supported by Joachim Fritz, Holger Jensen and Martin Duddek from the State Authority for Mining, Energy and Geology of Lower Saxony (LBEG).

The authors are grateful for this support. The content of this publication is in the responsibility of the authors.

The project takes part in the framework of the joint Task 44/Annex 38 “Heat pump and solar” of the Solar Heating and Cooling program and the Heat Pump program of the International Energy Agency (www.iea-shc.org/task44/index.html).

7. References

BERTRAM, E. ; STEGMANN, M. ; ROCKENDORF, G.: Heat Pump Systems with Borehole Heat Exchanger and Unglazed PVT Collector. In: *Proceedings of the ISES Solar World Congress 2011*. Kassel, 2011

DIN EN 14511-3: Luftkonditionierer, Flüssigkeitskühlsätze und Wärmepumpen mit elektrisch angetriebenen Verdichtern für die Raumbeheizung und Kühlung - Teil 3: Prüfverfahren, Beuth (2008)

GEHLIN, S.: *Thermal Response Test - Method Development and Evaluation*. Lulea, Sweden, Lulea University of Technology, 2002

KOENIGSDORFF, R. ; FEUERSTEIN, P. ; RYBA, M.: GEO-SOLE Vergleichende hydrogeologische und anlagentechnische Bewertung von Wärmeträgerflüssigkeiten für oberflächennahe geothermische Anwendungen. In: *Tagungsband 10. Internationales Anwenderforum Oberflächennahe Geothermie*. Regensburg : OTTI, 2010 — ISBN 9783941785120, pp. 58-65

KUSUDA, T. ; ACHENBACH, P. R.: *Earth Temperature and Thermal Diffusivity at Selected Stations in the United States* (National Bureau of Standards Report Nr. 8972) : National Bureau of Standards, 1965